Available online at www.CivileJournal.org

Civil Engineering Journal

(E-ISSN: 2476-3055; ISSN: 2676-6957)

Vol. 9, No. 06, June, 2023

Estimation of Soil Moisture for Different Crops Using SAR Polarimetric Data

K. Kanmani [1], Vasanthi P. [1*], Packirisamy Pari [2], N. S. Shafeer Ahamed [1]

[1] *Department of Civil Engineering, School of Infrastructure, B.S. Abdur Rahman Crescent Institute of Science and Technology, Vandalur, Chennai, Tamilnadu, 600 048, India.*

[3] *Associate Consultant, Darashaw & Company Private Limited, Tamilnadu, India.*

Received 15 March 2023; Revised 19 May 2023; Accepted 26 May 2023; Published 01 June 2023

Abstract

Soil moisture is an essential factor that influences agricultural productivity and hydrological processes. Soil moisture estimation using field detection methods takes time and is challenging. However, using Remote Sensing (RS) and Geographic Information System (GIS) technology, soil moisture parameters become easier to detect. In microwave remote sensing, synthetic aperture radar (SAR) data helps to retrieve soil moisture from more considerable depths because of its high penetration capability and the illumination power of its light source. This study aims to process the SAR Sentinel-1A data and estimate soil moisture using the Water Cloud Model (WCM). Many physical and empirical models have been developed to determine soil moisture from microwave remote sensing platforms. However, the Water Cloud Model gives more accurate results. In this study, the WCM model is used for mixed crop types. The experimental soil moisture was determined from in-situ soil samples collected from various agricultural areas. The soil backscattering values corresponding to the different soil sampling locations were derived from Sentinel SAR data. Using linear regression analysis, the laboratory's soil moisture results and soil backscattering values were correlated to arrive at a model. The model was validated using a secondary set of in-situ moisture content values taken during the same period. The R2 and RMSE of the model were observed to be 0.825 and 0.0274, respectively, proving a strong correlation between the experimental soil moisture and satellite-derived soil moisture for mixed crop field types. This paper explains the methodology for arriving at a model for soil moisture estimation. This model helps to recommend suitable crop types in large, complex areas based on predicted moisture content.

Keywords: Water Cloud Model (WCM); Synthetic Aperture Radar (SAR); Soil Backscattering.

1. Introduction

Soil moisture is the most influential factor causing surface runoff fluctuations and soil infiltration capacity [1, 2]. Soil moisture varies based on location and crops [3]. The in-situ measurements available to measure soil moisture are complex. However, with RS and GIS technology, we can estimate the soil moisture content for challenging areas such as highly vegetated areas, dense forests, and grasslands [4]. Active remote sensors such as RADAR transmit signals to the earth's surface by illuminating their own light source and receiving the signals that are reflected back to the sensor. SAR is an imaging radar that has its own energy source. The successive radar pulses from SAR are transmitted to the target, received back to the sensor as backscattered signals, and then recorded. The spatial resolution of this image depends on pulse length and beam width.

* Corresponding author: vasanthi@crescent.education

http://dx.doi.org/10.28991/CEJ-2023-09-06-08

Radar backscattered energy depends on satellite sensor parameters and earth terrain parameters. Some sensor parameters include frequency/wavelength, polarization, viewing geometry, spatial resolution, and speckle. The earth's terrain parameters are the surface geometry, the roughness of the surface, and the dielectric constant. Among these factors, polarization, surface roughness, and dielectric properties play a dominant role in retrieving soil moisture content [5]. The polarization of the radar has a significant effect on the nature and magnitude of the backscattered signal. There are four combinations of polarization, which include both transmit and receive polarizations. They are HH, VV, VH, and HV. The letters H and V are designated as horizontal and vertical, respectively. HH and VV polarizations are like-polarized, whereas HV and VH are cross-polarized. The strength of like-polarized signals is stronger than that of cross-polarized signals.

The surface roughness of earth objects purely depends on the wavelength and incidence angle of RADAR [6]. The texture of the earth's surface is classified as smooth and rough. If the variations in the height of the objects (h) are smaller than the radar wavelength (λ) i.e., $h < \lambda$, then the surface is said to be smooth. When the variations in the height are greater than the radar wavelength i.e., $h > \lambda$, then the surface is said to be a rough surface [7]. The smooth surfaces appear darker in the radar image since very little energy is received back, and thus it is recorded by the radar antenna. The rough surfaces appear lighter in the radar image since more energy is scattered back to the radar antenna.

The dielectric properties of the soil surface are influenced by the percentage of moisture content in the soil [8]. The surface appears rougher and darker in the satellite image when the soil is moist or wet. The large difference in electric properties results in a higher radar backscattered signal [9]. However, if the soil is dry, the surface appears smooth and is lighter in color in the satellite image. Some transmitted energy penetrates the soil's subsurface, resulting in less backscattered energy.

In this study, the soil moisture values are determined using the backscattered energy of SAR data, which depends on polarization, surface roughness, and dielectric properties. The backscattered energy value of dual polarization (VV+VH) mode is used in this study. Many models, such as physical, empirical, and semi-empirical models [10], are used to determine soil moisture content. Many physical and empirical models are developed to simulate the data or parameters from microwave remote sensing platforms. However, these models are used only for a particular crop type.

The four different crop fields, such as paddy fields, sesame plants, groundnuts, and jasmine flowering plants, were selected to assess the soil moisture for different agricultural fields. The Water Cloud Model (WCM) is extensively used for the above different heterogeneous crop fields to explore the model's capabilities. The main aim of this study is to calculate the soil moisture content using the Water Cloud Model (WCM) for different heterogeneous agricultural fields such as paddy fields, sesame plants, groundnuts, and jasmine flowering plants.

In this study, the complex effect of scattering between vegetation and soil is made simple by the WCM model, which works for many vegetation layer types. The WCM model removes the scattering effect of vegetation layers to estimate soil moisture content.

2. Literature Review

Srinivasa Rao et al. [11] used the Dubois model and Topp's model with only HH polarization to estimate soil moisture. The backscattering coefficient values and dielectric constant from HH polarization were computed, and these values were correlated and simulated for cross-polarized signatures like HV. These output results of soil moisture are compared with field-observed data and then validated. This model provides accurate results in soil moisture monitoring using RISAT data only in different polarizations, such as HH and HV (in medium and coarse resolutions).

Thanabalan et al. [12] used dual-polarimetric RISAT-1 to determine soil moisture. They used Topps and the Modified Dubois Model (MDM) to assess soil moisture in Theni District. IRS LISS IV satellite data provided the land use/land cover classifications for various land categories. Thus, the backscattering values were first derived, and then the surface roughness values were measured as field measurements from the selected sample locations. These values were correlated using a linear regression analysis.

Mirsoleimani et al. [13] used the Modified Dubois Model (MDM) and Calibrated Integral Equation Model (CIEM) to estimate soil moisture and compare the results in their study area, Karaj Watershed, Iran. They have used the Sentinel-1 C band in their study. The model (MDB and CIEM) variables include the angle of incidence and root mean square height, which are retrieved from the satellite images. The known values of in-situ observations were used as inputs to this model to correlate the backscattering values in the VV and VH polarizations. Then the correlated σ_0 values from Sentinel 1 SAR data were compared, and the results were validated using linear regression analysis.

Collingwood et al. [14] have used the ANN model for Melville Island, Nunavut's study area, to calculate soil moisture. They have used RADARSAT-2 SAR satellite data. The variables used in this study were the surface roughness values, the backscattered values of HH polarization, and the angle of incidence. The surface roughness variable was very dynamic and temporal. This model was applied to lower incidence angles to reduce the surface roughness and backscattered values in the study area.

Artificial neural network (ANN) models can be applied to more unique physical soil constraints [15]. Like conventional models, it is also used to retrieve soil moisture. But it gives better results than any other traditional model. This model is suitable for only studying the spatial distribution pattern of soil [16, 17]. ANNs must input the prior knowledge information into the model. Some statistical input data without any assumptions can be included in this model for analysis. These models can be applied to newer areas, requiring few assumptions [18].

Nijaguna et al. [19] employed an improved version of the Water Cloud Model (WCM) with a deep learning-based hybrid model to retrieve the soil moisture values. They have used the Deep Max Out Network (DMN) in addition to the Bidirectional Gated Recurrent Unit (Bi-GRU) schemes to attain higher accuracy in the results. This study suggested a novel technique as a hybrid model for soil moisture retrieval in homogenous regions.

Dopper et al. [20] have presented the hybrid technique of using radiative transfer modeling and machine learning with the help of hyperspectral images. They have applied this modeling technique to estimate soil moisture for permanent grassland sites. This modeling technique requires less number of field measurements. Also, the model yields good results for undisturbed and water-limited areas.

Lei et al. [21] have performed the vegetative canopy water content measurement to improve the Water Cloud Model (WCM) in retrieving soil moisture. Their results clearly stated that a more specific vegetation water content is created using the vertical canopy arrangement and biomass. Using Improved WCM (IWCM), the retrieval of soil moisture values for various levels of forests, such as green wood, grasslands etc., was determined.

Yahia et al. [22] have proposed the inversion of the Water Cloud Model (WCM) to enhance the measurement of soil moisture values. They have suggested using the Optical Trapezoidal Model (OTM) to compute vegetation canopy indices. They have applied this novel technique to the Sidi Rached and Blackwell farms.

Luo et al. [23] have used the Back Propagation Neural Network (BPNN) model to find the relationship between the bands and the soil moisture measurement data. The optical and thermal infrared satellite data from different periods were considered as input values, as were the field measurement data. They have applied this model to estimate the surface moisture content of the soil in bare land and vegetated areas. The correlation coefficient between the in-situ field-measured soil moisture and the estimated soil moisture was observed to be 0.9001, and the results give highly accurate values.

Based on the findings from the literature review, it is evident that soil moisture models are used only for specific agricultural fields or crop types like grasslands, wheat fields, or paddy fields. Hence, this study mainly estimates soil moisture for different crop fields or mixed heterogeneous crops. This study used Sentinel 1A SAR and microwave satellite data. Sentinel 1A has dual polarization (VV+VH) mode. Table 1 provides the specifications of the satellite data. The Water Cloud Model (WCM) is utilized in this study to find the moisture content in the soil for mixed heterogonous crop types. This model's main advantage is reducing the complex effect of scattering between vegetation and soil.

Table 1. Specifications of sentinel 1A SAR satellite data

Details of specification	Sentinel-1 data
Data product used	Ground Range Detected Level-1 Product
Orbit	Descending
Polarization	VV-VH
Imaging frequency	C-band (5.4GHz)
Resolution	20 m (Full resolution)
Temporal Resolution	12 days

3. Study Area and Data Collection

The study area chosen is Maiyur and Sampathinallur villages, Maduranthakam Taluk, Kancheepuram district, Tamil Nadu, India. This area has a hot and humid climate. The Palar River is the major river in this region, which is not perennial. Generally, these villages have witnessed average rainfall and have more diversified agricultural crop fields. The average temperature in this area ranges from 19.8 to 38.6 ºC.

The study area extends from 12°40'31.57"N, 79°56'13.43"E to 12°39'52.43"N, 79°56'33.27"E. The study area is shown in Figure 1.

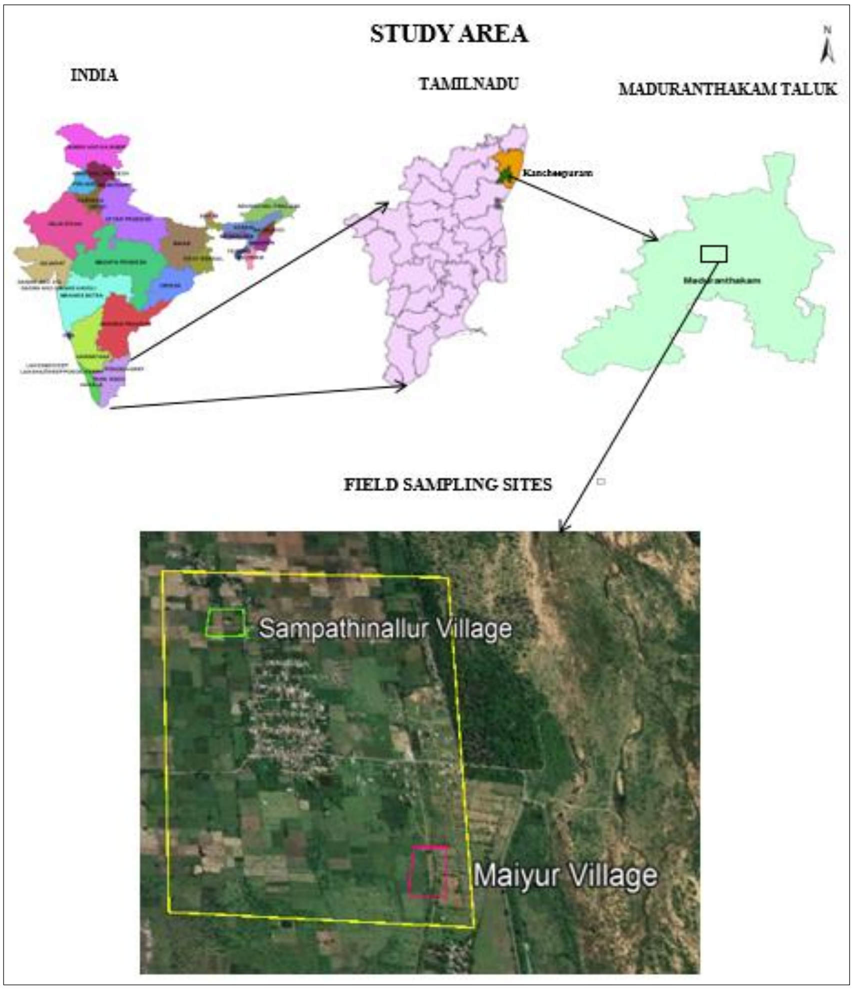

Figure 1. The study area of Maiyur and Sampathinallur village

Fourteen soil samples were collected from the study area during February 2022 and March 2022 at four different agricultural fields in Maiyur and Sampathinallur villages in Maduranthakam taluk, Kancheepuram district, Tamil Nadu, India. Field 1 and Field 2 soil samples were collected from paddy fields and sesame plants, respectively, at Maiyur village. Field 3 and Field 4 soil samples were collected from groundnut and jasmine flowering plants, respectively, at Sampathinallur village. The eight in-situ soil samples were used for estimating the experimental soil moisture measurement, and the remaining six ground samples were utilized for validating the model. The spatial location of in-situ soil samples is depicted in Figure 2.

(a) Maiyur Village (b) Sampathinallur village

Figure 2. Field sample data Locations

The soil samples were collected from Maiyur and Sampathinallur villages on the same date as the satellite passed the study region. The Global Positioning System was used to determine the location of the soil samples [24]. Figure 3 shows the photos taken in the field while collecting the soil samples.

Figure 3. Soil sampling

The gravimetric soil moisture content of the field samples was determined. Volumetric soil moisture has been determined from gravimetric soil moisture [25]. The following formula is used to compute both gravimetric and volumetric soil moisture:

$$S_g = \frac{Ws - Wd}{Wd} \tag{1}$$

$$\rho_b = \frac{Ws}{V} \tag{2}$$

$$S_v = S_g \times \rho_b \tag{3}$$

where S_g is Gravimetric soil moisture in cm^3/cm^3, ρ_b is Bulk Density in gm/cm^3, S_v is Volumetric Soil moisture in cm^3/cm^3, W_s is Weight of wet sample in gm, W_d is Weight of dried sample in gm, and V is Volume of sample in cm^3.

The gravimetric soil moisture values of the collected soil samples are tabulated in Table 2. The gravimetric moisture content lies between 0.099 cm^3/cm^3 and 0.169 cm^3/cm^3. The observations show that the soil moisture content is very low at the S13 and S14 site samples in Field4 compared to other field site samples.

Table 2. Experimental results of field sample data

Sl. No.	Sample_ID	Latitude	Longitude	Gravimetric soil moisture (cm^3 cm^{-3})
1	F1_S1	12°39'56.44"N	79°56'34.07"E	0.127
2	F1_S2	12°39'56.42"N	79°56'33.53"E	0.147
3	F1_S3	12°39'55.39"N	79°56'33.36"E	0.133
4	F1_S4	12°39'55.21"N	79°56'33.84"E	0.132
5	F2_S5	12°39'54.22"N	79°56'33.73"E	0.157
6	F2_S6	12°39'54.35"N	79°56'33.10"E	0.169
7	F2_S7	12°39'52.61"N	79°56'32.72"E	0.146
8	F2_S8	12°39'52.43"N	79°56'33.27"E	0.136
9	F3_S9	12°40'30.25"N	79°56'13.41"E	0.146
10	F3_S10	12°40'29.74"N	79°56'13.40"E	0.141
11	F3_S11	12°40'29.80"N	79°56'15.24"E	0.131
12	F3_S12	12°40'30.26"N	79°56'15.22"E	0.143
13	F4_S13	12°40'30.47"N	79°56'14.38"E	0.116
14	F4_S14	12°40'31.57"N	79°56'13.43"E	0.099

4. Research Methodology

The Sentinel Application Platform (SNAP) software is used to process the sentinel SAR data in this study. In the Sentinel Application Platform (SNAP), the Sentinel data is opened as an XML file with the band combinations B4, B3, and B2. The sentinel 1A SAR is pre-processed in the SNAP toolbox. The amplitude and intensity values of VV and VH scenes could be viewed on the display. Generally, all the bands in the Sentinel data were of different sizes and resolutions. The subset function is used to perform both spatial and spectral resampling. The resampling technique is performed to make all the bands of the same size and resolution. Lee's adaptive filter does the speckle suppression in SAR data. SRTM DEM data is used for terrain correction. Figure 4 displays the sentinel 1A SAR data used in this study. The False Color Composite (FCC) of different polarizations of the satellite is viewed in the display.

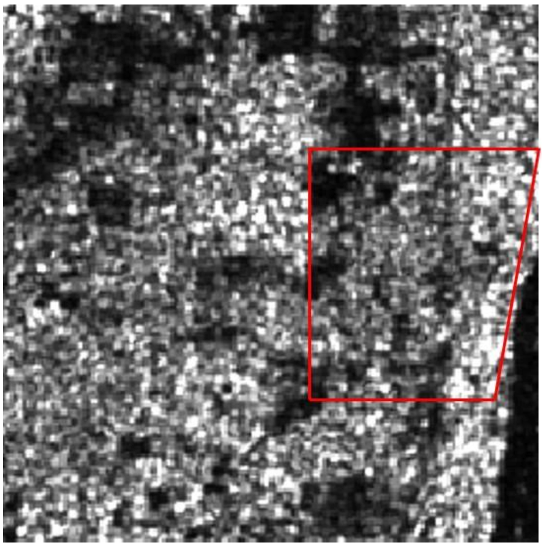

Figure 4. Sentinel 1A SAR data of study area

The backscattering values are retrieved from SAR data, representing the vegetation and underlying soil [26]. The values of soil backscattering are extracted from the combined backscattered energy [27]. The methodology of this study is shown in Figure 5.

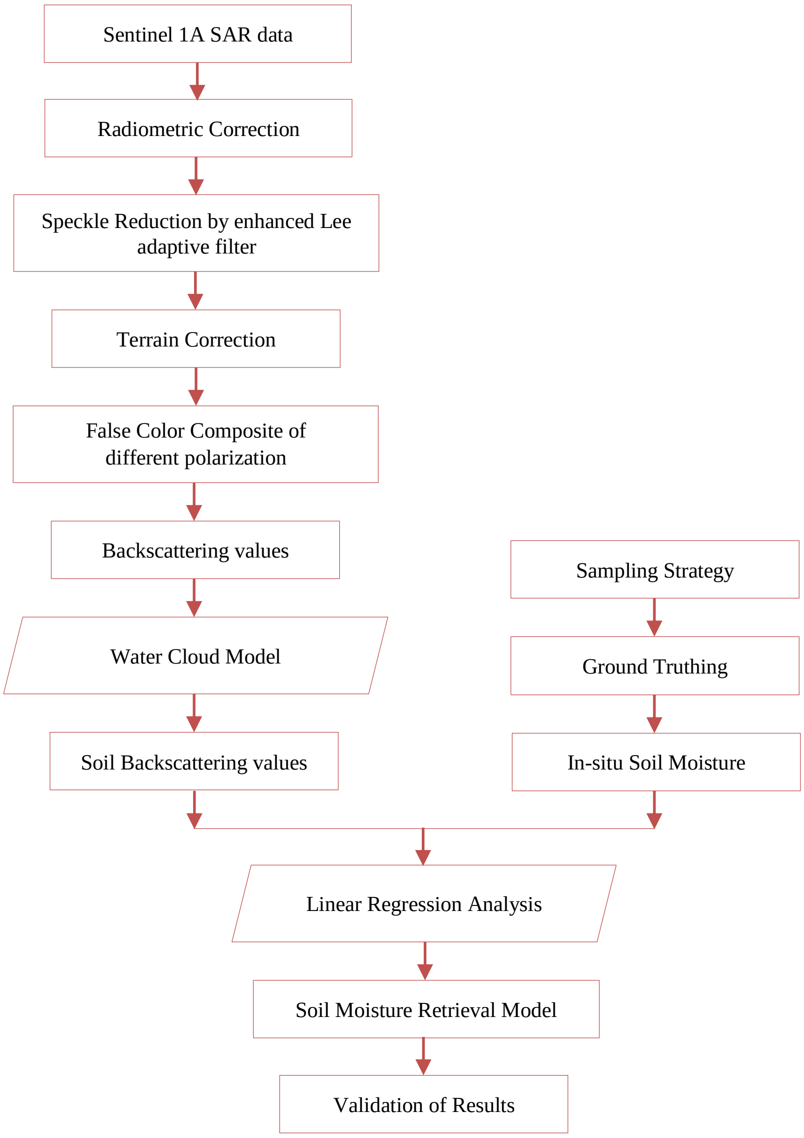

Figure 5. Methodology for Sentinel data processing and soil moisture retrieval

Using WCM, the soil moisture values are then retrieved from the combined backscattering value. The relationship between combined backscattering of vegetation & soil is given below [28].

$$\sigma^0 = \sigma^0 veg + \tau^2 \sigma^0 soil \tag{4}$$

$$\sigma^0 veg = A\, m_v cos\theta\ (1 - \tau^2) \tag{5}$$

$$\tau^2 = e^{(-2Bm_v\, sec\theta)} \tag{6}$$

where σ^0 is combined backscattering value, $\sigma^0 veg$ is vegetation backscattering value, $\sigma^0 soil$ is soil backscattering value, m_v is vegetation water content, θ is local incidence angle that is extracted from the corrected SAR data, and τ^2 is two-way vegetation transmissivity.

The vegetation moisture content (m_v) is determined from the laboratory method and is employed in the WCM [29]. These values from the model represent the combined backscattering values. The linear regression analysis is then carried out, which proposes a statistical model to determine the soil moisture parameter for the respective soil backscattering values for heterogeneous crops. The in-situ soil moisture values and the soil backscattering values are correlated using a linear regression model. The experimental soil moisture values were compared and analyzed with the satellite-derived soil moisture values to validate the model using a secondary set of in-situ soil samples.

5. Results and Discussion

A regression analysis was performed between the soil backscattering values and in-situ soil moisture values. Table 3 shows the soil backscattering values from the sentinel SAR data. From the regression analysis, the correlation coefficient value (R^2) is found to be 0.825, as depicted in Figure 6. Thus, there is a good correlation between satellite-derived soil backscattering and experimental soil moisture values [30].

Table 3. Experimental results and satellite-derived soil backscattering values of field sample data

Sl. No.	Sample_ID	Experimental soil moisture ($cm^3\ cm^{-3}$)	Soil backscattering values in dB
1	F1_S1	0.244	-13.421
2	F1_S3	0.254	-12.544
3	F2_S5	0.312	-14.269
4	F2_S7	0.292	-14.034
5	F3_S9	0.297	-13.924
6	F3_S11	0.266	-13.922
7	F3_S12	0.291	-14.470
8	F4_S14	0.167	-11.725

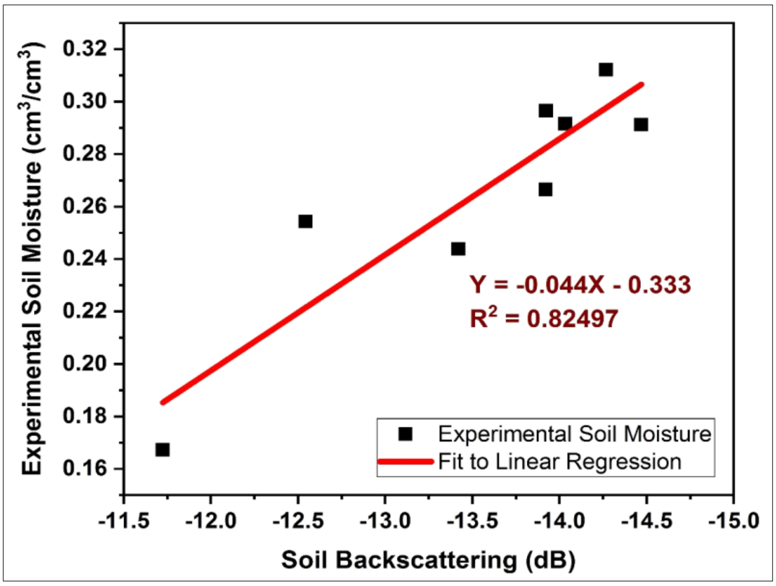

Figure 6. Regression Analysis between experimental soil moisture and soil backscattering values

From the linear statistical regression analysis, the soil moisture for heterogeneous crops can be obtained from the equation;

$$\text{Soil Moisture} = (-0.044 * \sigma^0 soil) - 0.333 \tag{7}$$

The satellite-derived and the measured soil moisture values are compared and analyzed to validate the above equation. The Root Mean Square Error (RMSE) value is determined to be 0.0274 [31]. Figure 7 compares the observed field values and satellite-derived soil moisture.

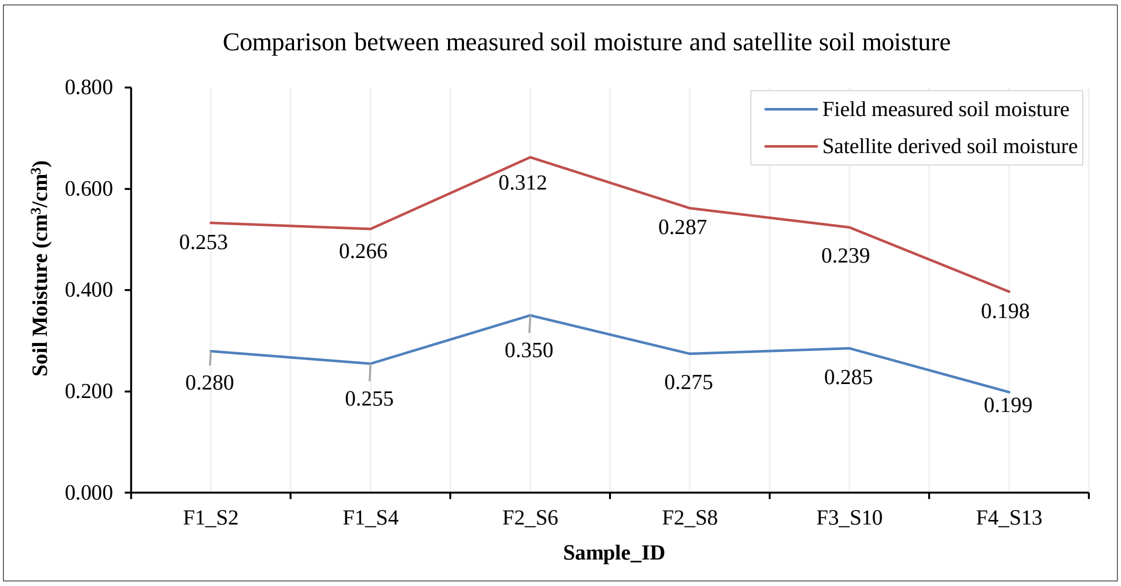

Figure 7. Comparison between field and satellite-derived soil moisture

The R^2 and RMSE of observed and derived values obtained from the model are 0.825 and 0.0274, respectively. The deviation from the field and satellite-based soil moisture values is between 0.01 cm^3/cm^3 to 0.04 cm^3/cm^3. This model was validated by comparing the soil moisture values obtained from the field and the model. The results prove that the proposed model can be applied to different agricultural fields. Thus, the proposed model is also applicable for estimating the soil moisture for various crop fields. This model can be used to reduce the oversupply of water for agricultural purposes and to alleviate the water shortage in particular locations based on soil moisture.

The R^2 value reported by various researchers was between 0.65 and 0.78, and the RMSE value ranged from 0.05 to 1. The backscattered values purely depend on the vegetation over the underlying soil and the surface roughness. Due to the effects of the physical parameters that affect the backscattered signal, the results of their findings were low. The results retrieved from Figure 7 are accurate when compared to other earlier studies.

6. Conclusion

This study estimates the soil moisture for different crop fields using Remote Sensing and GIS technology. Using Setinel-1 SAR data, a semi-empirical WCM model has been used in this study to determine the soil moisture values from SAR backscattering values [32]. The regression analysis shows that soil moisture has a robust correlation with the satellite-derived soil backscattering values. The same model may be further applied for more mixed land cover. This model is more suitable for heterogeneous crop regions. The results from this model can be used for irrigation management practices so that a sufficient quantity of water may be irrigated for the crops in that region to attain maximum crop productivity yield. These results will be more beneficial for using water resources in the area to increase the crop productivity index.

The processing of the Sentinel-1 data and the assessment of soil moisture initially had several limitations. Soil moisture estimation is more complex in highly vegetated areas when compared with dry, bare soil areas. The satellite backscattered signals are more affected by surface roughness, dielectric constant, and vegetation cover over the underlying soil [33]. The effect of these parameters results in more complexity in extracting the satellite backscattered signals. The resulting backscattered energy is the combination of both soil and vegetation backscattering values. To overcome these limitations, factors like vegetation moisture content and the Normalized Difference Vegetation Index (NDVI) are used in this study. More factors like the Normalized Difference Water Index (NDWI), Leaf Area Index (LAI), Enhanced Vegetation Index (EVI), etc. can be used for further study to assess the soil moisture content for more accurate results. In addition to Sentinel-1 SAR data, Sentinel-2 satellite data, which provides high spatial and temporal resolution, can be explored to assess soil moisture estimation [34]. The various regression models will be used for comparing the satellite-derived soil backscattering values and the experimental soil moisture.

7. Declarations

7.1. Author Contributions

Conceptualization, K.K.; methodology, K.K., V.P., and P.P.; software, K.K. and P.P.; validation, K.K., P.P., and N.S.S.A.; formal analysis, K.K.; writing—original draft preparation, K.K. and V.P.; writing—review and editing, K.K., V.P., and N.S.S.A.; supervision, V.P.; project administration, V.P. All authors have read and agreed to the published version of the manuscript.

7.2. Data Availability Statement

Data sharing is not applicable to this article.

7.3. Funding

The authors received no financial support for the research, authorship, and/or publication of this article.

7.4. Acknowledgements

I would like to place my special thanks to my research supervisor Dr. Vasanthi Padmanabhan, Professor, Department of Civil Engineering, B.S. Abdur Rahman Crescent Institute of Science and Technology for her cooperation, guidance and support throughout this research work.

7.5. Conflicts of Interest

The authors declare no conflict of interest.

8. References

[1] Baghdadi, N., Holah, N., & Zribi, M. (2006). Soil moisture estimation using multi-incidence and multi-polarization ASAR data. International Journal of Remote Sensing, 27(10), 1907–1920. doi:10.1080/01431160500239032.

[2] Das, K., & Paul, P. K. (2015). Soil moisture retrieval model by using RISAT-1, C-band data in tropical dry and sub-humid zone of Bankura district of India. Egyptian Journal of Remote Sensing and Space Science, 18(2), 297–310. doi:10.1016/j.ejrs.2015.09.004.

[3] Baghdadi, N., Choker, M., Zribi, M., El Hajj, M., Paloscia, S., Verhoest, N. E. C., Lievens, H., Baup, F., & Mattia, F. (2016). A new empirical model for radar scattering from bare soil surfaces. Remote Sensing, 8(11), 920. doi:10.3390/rs8110920.

[4] Santi, E., Paloscia, S., Pettinato, S., Notarnicola, C., Pasolli, L., & Pistocchi, A. (2013). Comparison between SAR soil moisture estimates and hydrological model simulations over the Scrivia test site. Remote Sensing, 5(10), 4961–4976. doi:10.3390/rs5104961.

[5] Tao, L., Wang, G., Chen, X., Li, J., & Cai, Q. (2019). Estimation of soil moisture using a vegetation scattering model in wheat fields. Journal of Applied Remote Sensing, 13(04), 1. doi:10.1117/1.jrs.13.4.044503.

[6] Song, K., Zhou, X., & Fan, Y. (2010). Retrieval of Soil Moisture Content from Microwave Backscattering Using a Modified IEM Model. Progress In Electromagnetics Research B, 26, 383–399. doi:10.2528/pierb10072905.

[7] Sahadevan, D. K., Rao, S. S., & Pandey, A. K. (2019). Soil Moisture Monitoring with Dual-Incidence-Angle RISAT-1 Data: A Pilot Study from Vidarbha Region. Journal of the Indian Society of Remote Sensing, 47(9), 1497–1506. doi:10.1007/s12524-019-00998-4.

[8] Sanli, F. B., Kurucu, Y., Esetlili, M. T., & Abdikan, S. (2008). Soil moisture estimation from RADARSAT-1, ASAR and PALSAR data in agricultural fields of Menemen plane of western Turkey. International Society for Photogrammetry and Remote Sensing, 37, 75-81.

[9] Jackson, T. J., Schugge, T. J., Nicks, A. D., Coleman, G. A., & Engman, E. T. (1981). Soil moisture updating and microwave remote sensing for hydrological simulation. Hydrological Sciences Bulletin, 26(3), 305–319. doi:10.1080/02626668109490889.

[10] Oh, Y., Sarabandi, K., & Ulaby, F. T. (2002). Semi-empirical model of the ensemble-averaged differential Mueller matrix for microwave backscattering from bare soil surfaces. IEEE Transactions on Geoscience and Remote Sensing, 40(6), 1348–1355. doi:10.1109/TGRS.2002.800232.

[11] Srinivasa Rao, S., Dinesh kumar, S., Das, S. N., Nagaraju, M. S. S., Venugopal, M. V., Rajankar, P., Laghate, P., Reddy, M. S., Joshi, A. K., & Sharma, J. R. (2013). Modified Dubois Model for Estimating Soil Moisture with Dual Polarized SAR Data. Journal of the Indian Society of Remote Sensing, 41(4), 865–872. doi:10.1007/s12524-013-0274-3.

[12] Thanabalan, P., & Vidhya, R. (2018). Derivation of soil moisture using modified Dubois model with field assisted surface roughness on RISAT-1 data. Earth Sciences Research Journal, 22(1), 13–18. doi:10.15446/esrj.v22n1.59972.

[13] Mirsoleimani, H. R., Sahebi, M. R., Baghdadi, N., & El Hajj, M. (2019). Bare soil surface moisture retrieval from sentinel-1 SAR data based on the calibrated IEM and dubois models using neural networks. Sensors (Switzerland), 19(14), 3209. doi:10.3390/s19143209.

[14] Collingwood, A., Charbonneau, F., Shang, C., & Treitz, P. (2018). Spatiotemporal variability of arctic soil moisture detected from high-resolution RADARSAT-2 SAR Data. Advances in Meteorology, 2018, 1–17. doi:10.1155/2018/5712046.

[15] Said, S., Kothyari, U. C., & Arora, M. K. (2008). ANN-Based Soil Moisture Retrieval over Bare and Vegetated Areas Using ERS-2 SAR Data. Journal of Hydrologic Engineering, 13(6), 461–475. doi:10.1061/(asce)1084-0699(2008)13:6(461).

[16] Gopal, S., & Woodcock, C. (1996). Remote sensing of forest change using artificial neural networks. IEEE Transactions on Geoscience and Remote Sensing, 34(2), 398–404. doi:10.1109/36.485117.

[17] Angiuli, E., del Frate, F., & Monerris, A. (2008). Application of Neural Networks to Soil Moisture Retrievals from L-Band Radiometric Data. IGARSS, IEEE International Geoscience and Remote Sensing Symposium. doi:10.1109/igarss.2008.4778927.

[18] Mas, J. F., & Flores, J. J. (2008). The application of artificial neural networks to the analysis of remotely sensed data. International Journal of Remote Sensing, 29(3), 617–663. doi:10.1080/01431160701352154.

[19] Nijaguna, G. S., Manjunath, D. R., Abouhawwash, M., Askar, S. S., Basha, D. K., & Sengupta, J. (2023). Deep Learning-Based Improved WCM Technique for Soil Moisture Retrieval with Satellite Images. Remote Sensing, 15(8). doi:10.3390/rs15082005.

[20] Döpper, V., Rocha, A. D., Berger, K., Gränzig, T., Verrelst, J., Kleinschmit, B., & Förster, M. (2022). Estimating soil moisture content under grassland with hyperspectral data using radiative transfer modelling and machine learning. International Journal of Applied Earth Observation and Geoinformation, 110, 102817. doi:10.1016/j.jag.2022.102817.

[21] Lei, J., Yang, W., & Yang, X. (2022). Soil Moisture in a Vegetation-Covered Area Using the Improved Water Cloud Model Based on Remote Sensing. Journal of the Indian Society of Remote Sensing, 50(1), 1–11. doi:10.1007/s12524-021-01450-2.

[22] Yahia, O., Karoui, M. S., & Guida, R. (2022). An Inversion of a Modified Water Cloud Model for Soil Moisture Content Estimation Through Sentinel-1 and Landsat-8 Remote Sensing Data. IGARSS 2022 - 2022 IEEE International Geoscience and Remote Sensing Symposium. doi:10.1109/igarss46834.2022.9884192.

[23] Luo, D., Wen, X., & He, P. (2023). Surface Soil Moisture Estimation Using a Neural Network Model in Bare Land and Vegetated Areas. Journal of Spectroscopy, 2023, 1–10. doi:10.1155/2023/5887177.

[24] Neusch, T., & Sties, M. (1999). Application of the Dubois-model using experimental synthetic aperture radar data for the determination of soil moisture and surface roughness. ISPRS Journal of Photogrammetry and Remote Sensing, 54(4), 273–278. doi:10.1016/S0924-2716(99)00019-2.

[25] Pari, P., Thirumaraiselvan, P., Ramalingam, M., & Jayalakshmi, S. (2020). A statistical model for estimation of soil moisture in paddy field using microwave satellite data. Progress In Electromagnetics Research M, 94, 155–166. doi:10.2528/PIERM20051401.

[26] Polychronaki, A., Gitas, I. Z., Veraverbeke, S., & Debien, A. (2013). Evaluation of ALOS PALSAR imagery for burned area mapping in greece using object-based classification. Remote Sensing, 5(11), 5680–5701. doi:10.3390/rs5115680.

[27] Wang, H., Méric, S., Allain, S., & Pottier, E. (2014). Adaptation of Oh Model for soil parameters retrieval using multi-angular RADARSAT-2 datasets. Journal of Surveying and Mapping Engineering, 2(4), 65-74.

[28] Han, D., Liu, S., Du, Y., Xie, X., Fan, L., Lei, L., Li, Z., Yang, H., & Yang, G. (2019). Crop water content of winter wheat revealed with sentinel-1 and sentinel-2 imagery. Sensors (Switzerland), 19(18), 4013. doi:10.3390/s19184013.

[29] Clementini, C., Pomente, A., Latini, D., Kanamaru, H., Vuolo, M. R., Heureux, A., Fujisawa, M., Schiavon, G., & Frate, F. Del. (2020). Long-term grass biomass estimation of pastures from satellite data. Remote Sensing, 12(13), 2160. doi:10.3390/rs12132160.

[30] Ferencz, C., Bognár, P., Lichtenberger, J., Hamar, D., Tarcsai, G., Timár, G., Molnár, G., Pásztor, S., Steinbach, P., Székely, B., Ferencz, O. E., & Ferencz-Árkos, I. (2004). Crop yield estimation by satellite remote sensing. International Journal of Remote Sensing, 25(20), 4113–4149. doi:10.1080/01431160410001698870.

[31] Kumar, K., Arora, M. K., & Hariprasad, K. S. (2016). Geostatistical analysis of soil moisture distribution in a part of Solani River catchment. Applied Water Science, 6(1), 25–34. doi:10.1007/s13201-014-0202-x.

[32] Bai, X., & He, B. (2015). Potential of Dubois model for soil moisture retrieval in prairie areas using SAR and optical data. International Journal of Remote Sensing, 36(22), 5737–5753. doi:10.1080/01431161.2015.1103920.

[33] Cho, S., Jeong, J., Baik, J., & Choi, M. (2020). Soil moisture estimation based on water cloud model at the mountainous area. 40th Asian Conference on Remote Sensing, ACRS 2019: 14-18 October, 2019, Daejeon, South Korea.

[34] Bao, Y., Lin, L., Wu, S., Kwal Deng, K. A., & Petropoulos, G. P. (2018). Surface soil moisture retrievals over partially vegetated areas from the synergy of Sentinel-1 and Landsat 8 data using a modified water-cloud model. International Journal of Applied Earth Observation and Geoinformation, 72, 76–85. doi:10.1016/j.jag.2018.05.026.